

Effect of electron irradiation on vortex dynamics in $\text{YBa}_2\text{Cu}_3\text{O}_{7-\delta}$ single crystals

A.V.Bondarenko, A.A.Prodan

Karazin Kharkov National University, Physical Department, Svobody sq. 4, 61077 Kharkov, Ukraine, E-mail: Aleksander.V.Bondarenko@univer.kharkov.ua

Yu.T.Petrusenko, V.N.Borisenko

National Science Center "Kharkov Institute of Physics and Technology", Kharkov 61108, Ukraine

F.Dworschak, U.Dedek

Institut für Festkörperforschung Forschungszentrum Jülich GmbH, D-52425 Jülich, Germany

(October 24, 2018)

We report on drastic change of vortex dynamics with increase of quenched disorder: for rather weak disorder we found a single vortex creep regime, which we attribute to a Bragg-glass phase, while for enhanced disorder we found an increase of both the depinning current and activation energy with magnetic field, which we attribute to entangled vortex phase. We also found that introduction of additional defects always increases the depinning current, but it increases activation energy only for elastic vortex creep, while it decreases activation energy for plastic vortex creep.

PACS numbers: 74.60.Jg, 74.60.Ge, 74.60.Ec, 74.72.Bk

The effect of random pinning on crystalline order and on dynamics of the flux-line-lattice (FLL) was a subject of numerous experimental and theoretical investigations. Neutron diffraction [1] and μSR [2] experiments gave experimental evidence for the existence of two vortex solid phases with different positional correlations. Magnetization measurements [3] of $\text{Bi}_2\text{Sr}_2\text{CaCu}_2\text{O}_8$ showed that the field, H_{on} , at which a steep increase of the measured current $J_m(H)$ begins, coincides approximately with the field above which the intensity of Bragg peaks sharply decreases [1]. The field H_{on} was interpreted as a phase boundary between low field ordered and high field disordered vortex phases. These experimental results are supported by theoretical studies. It was shown that in presence of rather weak disorder the FLL retains a quasi-long-range order resulting in the so-called Bragg glass phase [4]. However, with the increase of random pinning or magnetic field a transition to strongly disordered entangled vortex phase (glass phase) is predicted [5,6]. A sharp increase in magnetization below the fish-tail peak position H_p was observed in $\text{Nd}_{1.85}\text{Ce}_{0.15}\text{CuO}_{4-d}$ [7] and non twinned $\text{YBa}_2\text{Cu}_3\text{O}_{7-\delta}$ [8] single crystals.

Magnetic measurements showed that in optimally doped $\text{YBa}_2\text{Cu}_3\text{O}_{7-\delta}$ crystals no fishtail behavior is observed both in detwinned [9] and twinned [10] samples, while decrease of the oxygen content always induced non monotonous $J_m(H)$ -curves. Two distinctive peculiarities in the magnetization curves of oxygen deficient [10] and electron irradiated [11] crystals were observed: (1) the peaks H_{on} and H_p shift toward lower magnetic fields with increasing defect concentration, and (2) in magnetic fields $H < H_p$ the current J_m increases, while in magnetic fields $H > H_p$ the current J_m decreases with increasing defect concentration. It is believed [12,13] that the peak H_p separates elastic vortex creep in low and plastic vortex creep, mediated by motion of the FLL dislocations, in

high magnetic fields. Thus the introduction of additional defects leads to an increase of vortex pinning in the region of elastic creep and such behavior is expected. On the other hand, decrease of pinning force with increasing disorder observed in the region of plastic creep is non trivial, and reasons of such behavior are not known. The aim of this paper is to show the effect of point-like defects concentration on vortex dynamics and pinning parameters in $\text{YBa}_2\text{Cu}_3\text{O}_{7-\delta}$ single crystals.

The investigated sample was $\text{YBa}_2\text{Cu}_3\text{O}_{7-\delta}$ single crystal with $T_c \approx 93.5$ K and $\Delta T_c < 0.5$ K. Twin planes (TP's) inside the measured part of the sample were aligned in one direction. The transport current was applied along the ab -plane and at an angle $\alpha = 45^\circ$ with respect to TP's. Measurements were performed in magnetic fields applied parallel to the c -axis. Temperature stability of the sample during measurements was better than 5 mK, and measurements in the normal state showed that overheating of the sample at the highest dissipation level of $50 \mu\text{W}$ did not exceed 10 mK.

Additional defects were introduced by irradiation with 2.5-MeV electrons, which are suitable for production of point-like defects. Irradiation was performed at temperatures $T \leq 10\text{K}$ [14] and after irradiation the current-voltage characteristics (CVC) were measured without heating the sample above 110 K. This excludes diffusion, and therefore annihilation and clustering of the defects. Irradiation was performed at dose rate $4.2 \times 10^{13} \text{cm}^{-2} \text{sec}^{-1}$ and at an angle 5° off the c -axis to avoid electron channeling. Homogeneity of electron beam was about 5%. Following procedure used in Ref. [15] we estimated that irradiation dose 10^{18}cm^{-2} produces the averaged over all sublattices concentration of the defects 10^{-4} dpa, and that the penetration range $\sim 1\text{mm}$ is at least two orders higher than thickness of the crystal $\cong 7\mu\text{m}$ resulting in homogeneity of the defects along the c -axis

better than 1%. Reduction of the T_c after irradiation was $\Delta T_{irr} = 0.65, 1$ and 1.3 K after irradiation with doses $10^{18}, 2 \times 10^{18}$ and $3 \times 10^{18} \text{el/cm}^2$, respectively.

Fig.1 shows field variation of the measured "critical" current J_m determined at an electric field level 10^{-6}V/cm . Before irradiation the current J_m continuously decreases with increasing field as it was previously observed by Zhukov et al. in crystals with very small oxygen deficiency, $\delta \simeq 0.03$ [10]. After irradiation the $J_m(H)$ curves show fish-tail behavior and the peak position H_p in the $J_m(H)$ curves shifts toward low fields with the dose. It is also seen that introduction of additional defects increases J_m for $H < H_p$, while the current J_m decreases with the dose for $H > H_p$. Such variation of the J_m and H_p with increasing of the defect concentration is analogous to the behavior previously observed in oxygen deficient [10] and in electron irradiated [11] $\text{YBa}_2\text{Cu}_3\text{O}_{7-\delta}$ single crystals.

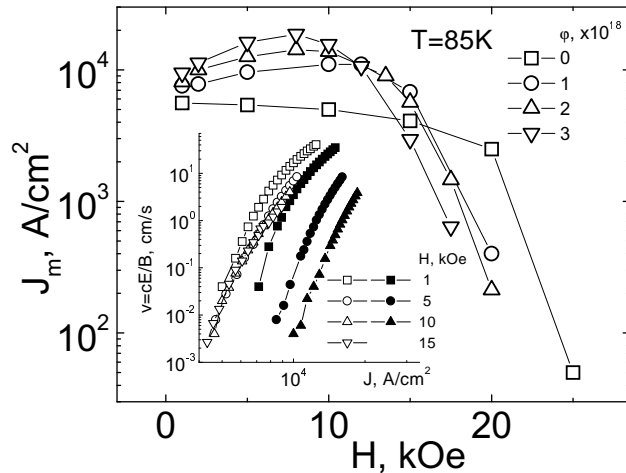


FIG. 1. Field variation of the current J_m . The inset shows vortex velocity versus J before (open symbols) and after (dark symbols) irradiation with $\varphi = 10^{18} \text{el/cm}^2$.

In low magnetic fields ($H \leq 15 \text{kOe}$ for non irradiated sample, and $H < H_p$ for irradiated samples) the CVC data follow the dependence [16]

$$E = E_0 \exp[-(U_0/kT)(J_c/J)^\mu], \quad (1)$$

where the exponent $\mu \simeq 1$, E_0 is a constant, U_0 is the activation energy, and k is the Boltzmann constant. The depinning critical current J_c can be determined by extrapolation of the ratio $\rho_d(J)/\rho_{BS}$ to unity [13] assuming that at current density $J = J_c$ the differential resistivity $\rho_d \equiv dE/dJ$ equals the flux flow resistivity in the Bardeen-Stephen model, $\rho_{BS} = \rho_N B/B_{c2}$ [17], where ρ_N is the normal state resistivity. Induction of the upper critical field was estimated assuming that $B_{c2} = (dB_{c2}/dT)(T - T_c)$ with $dB_{c2}/dT = -2.5 \text{T/K}$ [18]. Field variation of the J_c is shown in the inset of Fig.2a. Substituting these values of J_c in Eq.1, and fitting exper-

imental $E(J)$ -curves by this equation we derived $U_0(H)$ dependence shown in the inset of Fig.2a.

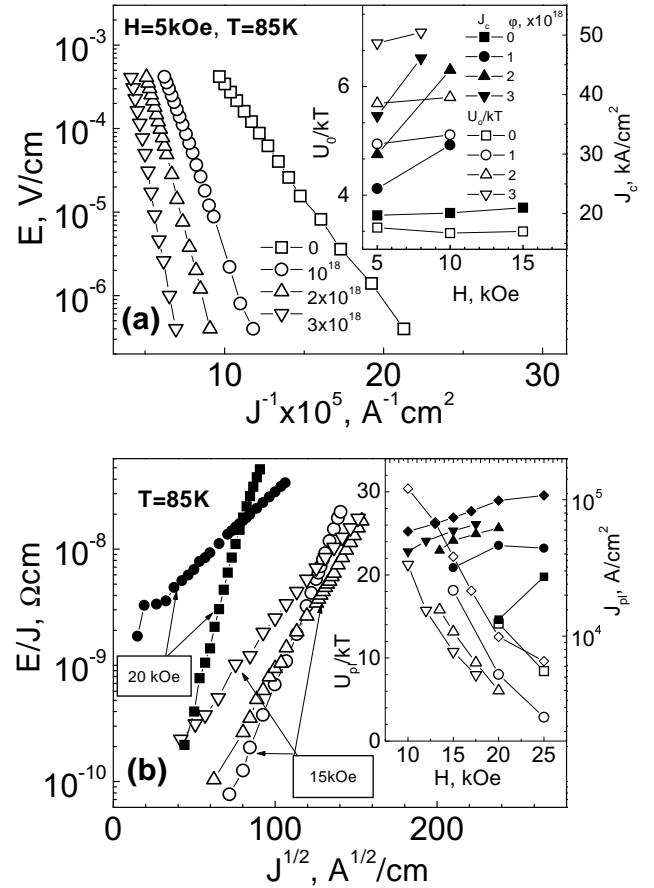


FIG. 2. (a) The $E(J)$ curves plotted as $E(J)$ vs. $1/J$. The inset shows field variation of the J_c and U_0 . (b) The $E(J)$ curves measured before (squares) and after irradiation with doses 10^{18} (circles), 2×10^{18} (up triangulars), and $3 \times 10^{18} \text{el/cm}^2$ (down triangulars), and plotted as $E(J)/J$ vs. $J^{1/2}$. The inset shows $J_{pi}(H)$ -dependence (dark symbols) and $U_{pi}(H)$ -dependence (open symbols) derived for $T = 85\text{K}$ before irradiation (squares) and after irradiation with doses 10^{18} (circles), 2×10^{18} (up triangulars), and $3 \times 10^{18} \text{el/cm}^2$ (down triangulars), and derived for $T = 82\text{K}$ and $\varphi = 3 \times 10^{18} \text{el/cm}^2$ (diamonds).

As one can see in Fig.1 and in the inset of Fig.2a, vortex dynamics, namely field variation of the pinning parameters, strongly depends on the strength of disorder. In presence of weak disorder (before irradiation) J_c , U_0 , and vortex velocity $v = cE/B$ do not depend on magnetic field indicating a single vortex creep regime, as it is predicted by the collective pinning theory [16] for low magnetic fields. Also, for this regime of vortex creep the current J_m decreases with increasing magnetic field due to increase of the flux density. Increase of the disorder induces field variation of the pinning parameters. After irradiation J_c and U_0 increase with magnetic field that leads to reduction of vortex velocity and to increase of

the current J_m with increasing magnetic field. These observations indicate that before and after irradiation we test different vortex phases.

In presence of weak quenched disorder the ordered Bragg-glass phase is expected [4] and our experimental data probably indicates that dynamics of just this vortex phase is described by the single vortex creep regime. Also note, that derived exponent $\mu \cong 1 \pm 0.15$ is close to the value of $\mu \cong 0.7 - 0.8$ predicted for the Bragg-glass phase for not too small currents [6]. With increase of disorder a transition of the Bragg-glass to entangled vortex phase is expected [5,6]. The derived after irradiation weak increase of the U_0 and rapid increase of the J_m with magnetic field correlates with previous experimental findings [8,11] for magnetic fields $B > B_{on}$, or in magnetic fields where the entangled vortex solid is expected. Therefore we believe that after irradiation we test the entangled vortex phase and dynamics of this phase is characterized by the increase of both J_c and U_0 with increasing magnetic field, which lead to rapid increase of the current J_m . Also, introduction of additional defects increases both the U_0 and J_c resulting in steep increase of the current J_m with irradiation dose, see Fig.1, in agreement with previous investigations [11,15].

Let us consider experimental data obtained in magnetic fields $H \geq 20kOe$ for nonirradiated sample, and in magnetic fields $H > H_p$ for irradiated samples. As one can see in Fig.2b, the CVC data follow the dependence predicted for motion of the FLL dislocations [12,19]

$$E(J) = \rho_0 J \exp\{-(U_{pl}/kT)[1 - (J_{pl}/J)^\mu]\}, \quad (2)$$

where $\mu = -1/2$, and ρ_0 is a constant. The main peculiarities of the curves presented in Fig.2b are that the slope of the curves measured in the same magnetic field decreases with increasing defects concentration and that these curves intersect one another. For vortex creep described by Eq.2 such behavior is possible only in that case when the critical current increases, but the activation energy decreases with increasing defect concentration. Extrapolating the ratio $\rho_d(J)/\rho_{BS}$ to unity we derived field and temperature variation of the current J_{pl} shown in the inset of Fig.2b and in Fig.3a, respectively. Substituting these values of J_{pl} in Eq.2, and fitting experimental $E(J)$ -curves by this equation we determined the field and temperature variation of U_{pl} shown in the inset of Fig.2b and in Fig.3a, respectively.

The current J_{pl} is determined by the interaction of the dislocations with the FLL and random pinning centers. Interaction with the FLL results in a shear limited contribution [20] $J_{sh} \propto c_{66}/Bd \propto B^{1/2}$, where $c_{66} = \Phi_0 B / (8\pi\lambda)^2$ is the shear modulus, Φ_0 is the flux quantum, λ is the penetration depth, $d \approx a_0$ is the width of channel for moving dislocation, and $a_0 \approx (\Phi_0/B)^{1/2}$ is the intervortex distance. As one can see in the inset of Fig.2b, in magnetic fields not very close to the melting point the current J_{pl} really increases with the field

in agreement with theoretical predictions. In the presence of random pinning the shear modulus c_{66} decreases [21] and therefore J_{sh} also decreases. However, the contribution of the core pinning increases with the defect concentration [16]. The derived increase of the current J_{pl} with irradiation dose indicates that increase of the core pinning dominates over reduction of the J_{sh} .

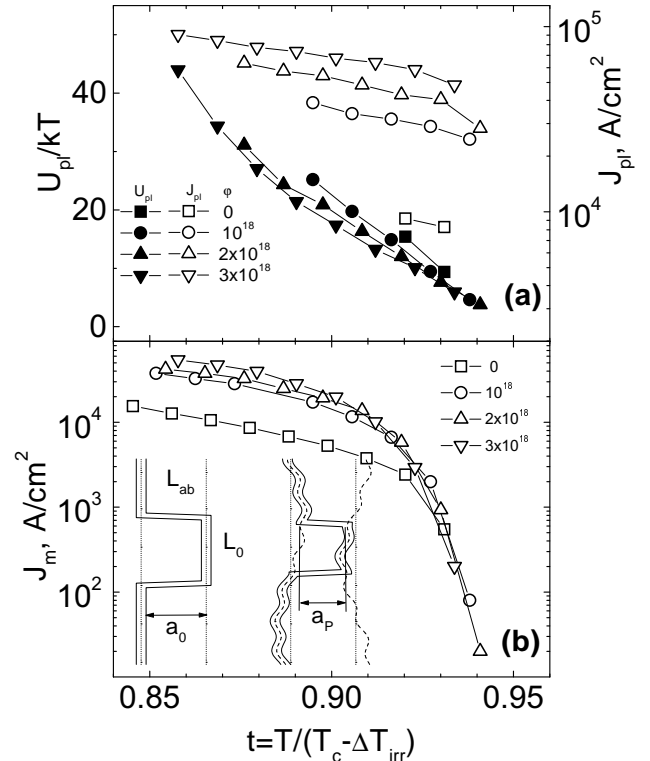


FIG. 3. (a) Temperature variation of U_{pl} and J_{pl} for $H = 15kOe$. (b) Temperature variation of J_m for $H = 15kOe$. The inset shows nuclei for the plastic creep in the absence (left) and in the presence (right) of random pinning.

The activation energy U_{pl} decreases with the increase of both irradiation dose and magnetic field. A decrease of the activation energy with increasing field agrees with theoretical calculations, $U_{pl} \approx \varepsilon \varepsilon_0 a_0 \propto B^{-1/2}$ [22], where $\varepsilon_0 = (\Phi_0/8\pi\lambda)^2$, and previous experimental findings [12,13]. But, a decrease of the activation energy with increasing irradiation dose is not evident. Of course, the T_c decreases after irradiation which leads to an increase of the $\lambda(T) = \lambda(0)/[1 - (T/T_c)^2]^{1/2}$, and hence to a decrease of the activation energy $U_{pl} \propto \lambda^{-2}$. However, the reduction of the T_c can not describe the fast decrease of U_{pl} in our measurements. This is demonstrated in Fig.3a, which shows dependence U_{pl} vs. $t \equiv T/(T_c - \Delta T_{irr})$. It is evident that U_0 decreases with the dose increasing even if we take into account the reduction of T_c .

To explain this behavior let us consider a displacement of a vortex segment L_0 over intervortex distance a_0 as shown in the left-hand inset of Fig.3b. In the absence of random pinning the energy of such nucleus can be writ-

ten as $U_{pl} = 2E_{el} + E_{pl}$, where $E_{el} \approx \varepsilon\varepsilon_0a_0$ is elastic energy of the vortex segment L_{ab} , and E_{pl} is the energy required for displacement of the vortex segment L_0 over the distance a_0 . At small driving forces such a nucleus is stable when $E_{pl} \geq 2E_{el}$. Thus we obtain a minimal activation energy $U_{pl} \approx 4\varepsilon\varepsilon_0a_0$, which coincides within a factor 4 with previous estimates $U_{pl} \approx \varepsilon\varepsilon_0a_0$ [22]. In the absence of random pinning the equilibrium positions of the vortices are the straight lines as it is shown by two parallel straight lines. In the presence of random pinning the equilibrium positions become curved as shown by dashed lines in the right-hand inset of Fig.3b. Therefore, along the vortex lines a vortex fragments, for which an average distance a_p between two neighboring equilibrium positions of vortex lines is smaller than a_0 appear. In this case the energy $U_{pl} \approx 4\varepsilon\varepsilon_0a_p$ is smaller than activation energy in the absence of pinning because $a_p < a_0$. Substantial displacements of vortex segments, $\Delta a_0 = a_0 - a_p \simeq 0.2a_0 \simeq 8nm$, due to core interaction with individual pinning centers probably unreliable, and we attribute them to fluctuations of the defects concentration, which naturally present in real crystals. Indeed, equating the work $A = J_{pl}F_0L_0a_p/c$, required for displacement of the segment L_0 over distance a_p , to the elastic energy, $2E_{el} = U_{pl}/2$, we estimated $L_0 \cong 500$ nm for $\varphi = 10^{18}$ el/cm², and derived that for coherence length $\xi(85K) = 5$ nm the segment L_0 interacts with about 200 point defects. Therefore, fluctuations of the defects concentration of 10% can give difference in core interaction with about 20 point defects in different positions of the segment L_0 .

TPs strongly affect pinning and dynamics of vortices [23–25]. In particular, being plane defects they form channels of easy vortex motion along the plane of twins [24,25]. Due to suppression of superconducting order parameter within the TPs some part of vortices is trapped by the TPs [26], and pinning of these vortices along the TPs may be reduced as compared with pinning in the bulk of the crystal [24]. Therefore, for the same driving force velocity of the trapped vortices can be higher compared with velocity of vortices placed in the bulk of crystal. In high magnetic fields contribution of the trapped vortices to dissipation of energy is small due to small fraction of these vortices. However, in a magnetic field 1 kOe the intervortex separation $a_0 \cong 140nm$ becomes comparable with the distance between twins $d \cong 300nm$ in our sample, and a significant part of vortices can be trapped by the TP's. Therefore, contribution of the trapped vortices increases with decreasing magnetic field, and deviation from the field scaling for non irradiated sample in low fields presented in the inset of Fig.1 probably reflects the reduced pinning of the trapped vortices.

In conclusion, we have shown that vortex dynamics dramatically depends on the strength of disorder. In presence of weak disorder a single vortex creep is realized, which we attribute to dynamical property of the

ordered Bragg-glass phase. In presence of strong disorder and for elastic vortex creep we have found rapid increase of the depinning current and weak increase of the activation energy with increasing magnetic field, which we attribute to dynamical property of the entangled vortex solid. We also found that the introduction of additional defects always increases the depinning critical current, but it increases the activation energy only for the elastic vortex creep, while it decreases the activation energy for the plastic vortex creep.

We gratefully acknowledge support by German Federal Ministry for Research and Technology under the Project UKR-032-96.

-
- [1] R. Cubitt et al., Nature **365** (1993) 407.
 - [2] S.L. Lee et al., Phys. Rev. Lett. **71** (1993) 3862.
 - [3] B. Khaykovich et al., Phys. Rev. Lett. **76** (1996) 2555.
 - [4] T. Giamarchi and P. Le Doussal, Phys. Rev. Lett. **72** (1994) 1530; T. Giamarchi and P. Le Doussal, Phys. Rev. **B52** (1995) 1242.
 - [5] D. Etras and D.R. Nelson, Physica **C272** (1996) 79; J. Kierfeld et al., Phys. Rev. **B55** (1997) 625; V. Vinokur et al., Physica **C295** (1998) 209.
 - [6] T. Giamarchi and P. Le Doussal, Phys. Rev. **B55** (1997) 6577.
 - [7] D. Giller et al., Phys. Rev. Lett. **79** (1997) 2542.
 - [8] T. Nishizaki, Phys. Rev. **B58** (1998) 11169; D. Giller et al., Phys. Rev. **B60** (1999) 106; M. Pissas et al., Phys. Rev. **B62** (2000) 1.
 - [9] A. Erb et al., J. Low Temp. Phys. **105** (1966) 1023.
 - [10] A.A. Zhukov et al., Phys. Rev. **B51** (1995) 12704; K. Deligiannis et al., Phys. Rev. Lett. **79** (1997).
 - [11] T. Nishizaki, Phys. Rev. **B61** (2000) 3649.
 - [12] Y. Abulafia et al., Phys. Rev. Lett. **77** (1996) 1596.
 - [13] A.V. Bondarenko et al., Phys. Rev. **B58** (1998) 2445.
 - [14] F. Dworschak et al., Physica **C235-240** (1994) 1343.
 - [15] J.Giapintzakis et al., Phys. Rev. **B45** (1992) 10672.
 - [16] G. Blatter et al., Rev. Mod. Phys. **66** (1994) 1125.
 - [17] J. Bardeen and M.J. Stephen, Phys. Rev. **A140** (1965) 1197.
 - [18] T.K. Worthington et al., Cryogenics **30** (1990) 417.
 - [19] J.P. Hirth and J. Lothe, Theory of Dislocations (John Wiley & Sons, New York, 1982), Chap 15.
 - [20] A. Pruijboom et al., Phys. Rev. Lett. **60** (1988) 1430.
 - [21] Y.J.M. Brechet et al., Phys. Rev. **B42** (1990) 2116.
 - [22] V.B. Geshkenbein et al., Physica **C162-164** (1989) 239.
 - [23] W.K. Kwok et al., Phys. Rev. Lett. **64** (1990) 966; S.Flesher et al., Phys. Rev. **B47** (1993) 14448.
 - [24] C. Duran et al., Nature **357** (1992) 474.
 - [25] A.I. Belyaeva et al., Solid State Commun. **85** (1993) 427;
 - [26] L.Y. Vinnikov et al., Superconductivity **3** (1990) 1120.